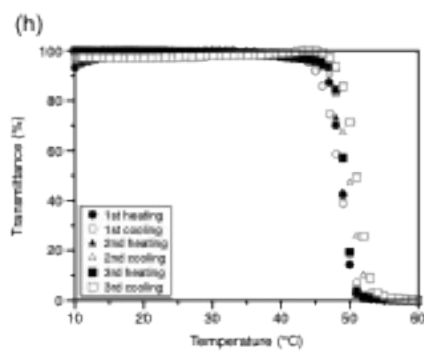
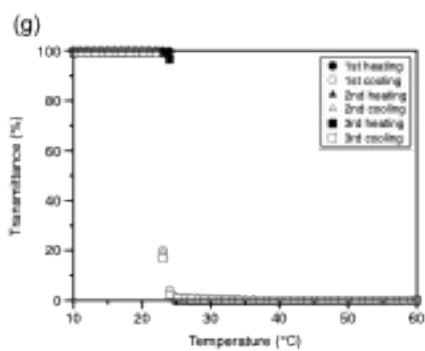
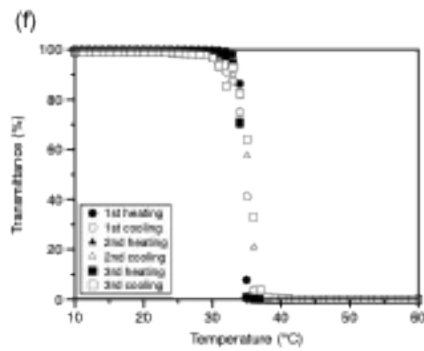
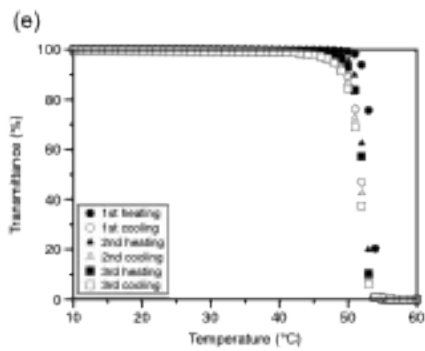
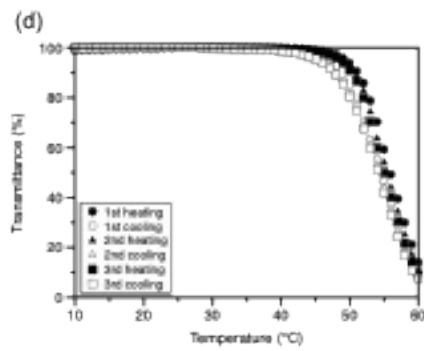
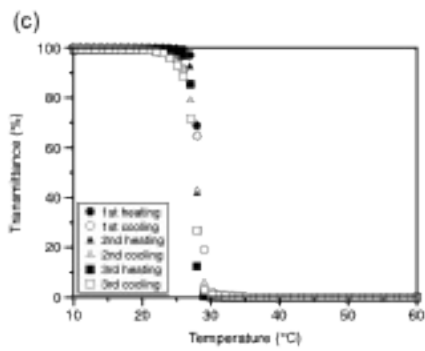
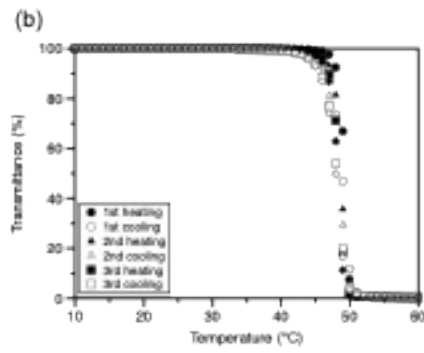
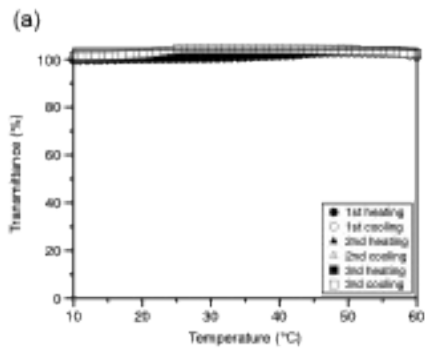


Figure S1. Transmittance curves of (a) 1 wt% and (b) 5wt% aqueous solutions of alkyl gallates measured at 500 nm. The temperature changed for 1 °C/min at the range of 10 to 60 °C.



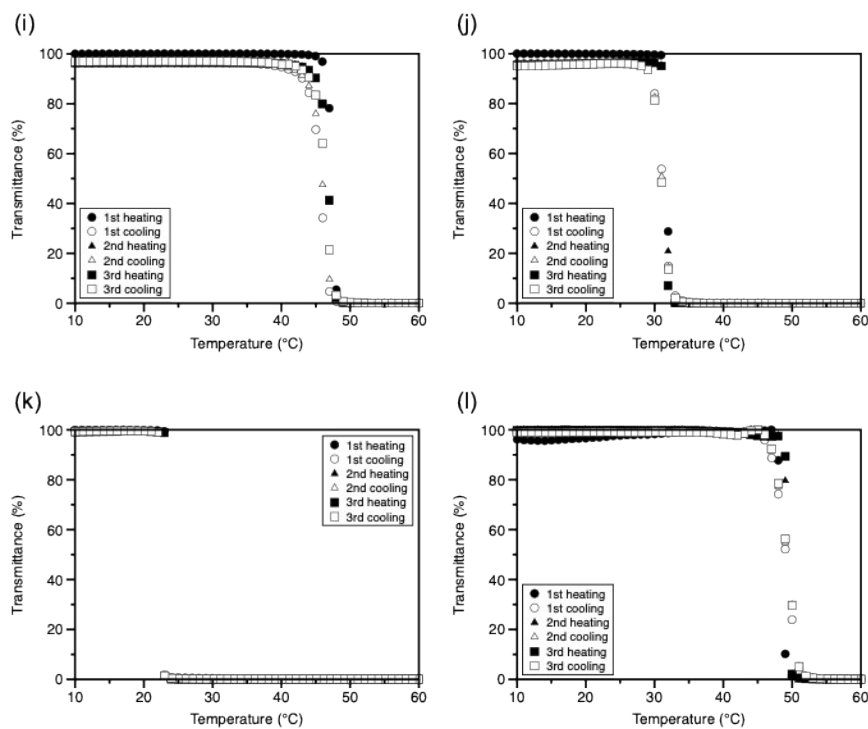


Figure S2. Transmittance curves of aqueous solutions of alkyl gallates measured at 500 nm during three consecutive heating and cooling cycles: (a) **Et-DEG** (1 wt%), (b) **Pr-DEG** (1 wt%), (c) **Bu-DEG** (1 wt%), (d) **Pr-TEG** (1 wt%), (e) **Et-DEG** (3 wt%), (f) **Pr-DEG** (3 wt%), (g) **Bu-DEG** (3 wt%), (h) **Pr-TEG** (3 wt%), (i) **Et-DEG** (5 wt%), (j) **Pr-DEG** (5 wt%), (k) **Bu-DEG** (5 wt%), and (l) **Pr-TEG** (5 wt%). The temperature was varied at a rate of $1\text{ }^{\circ}\text{C min}^{-1}$ over the range of 10–60 $^{\circ}\text{C}$.

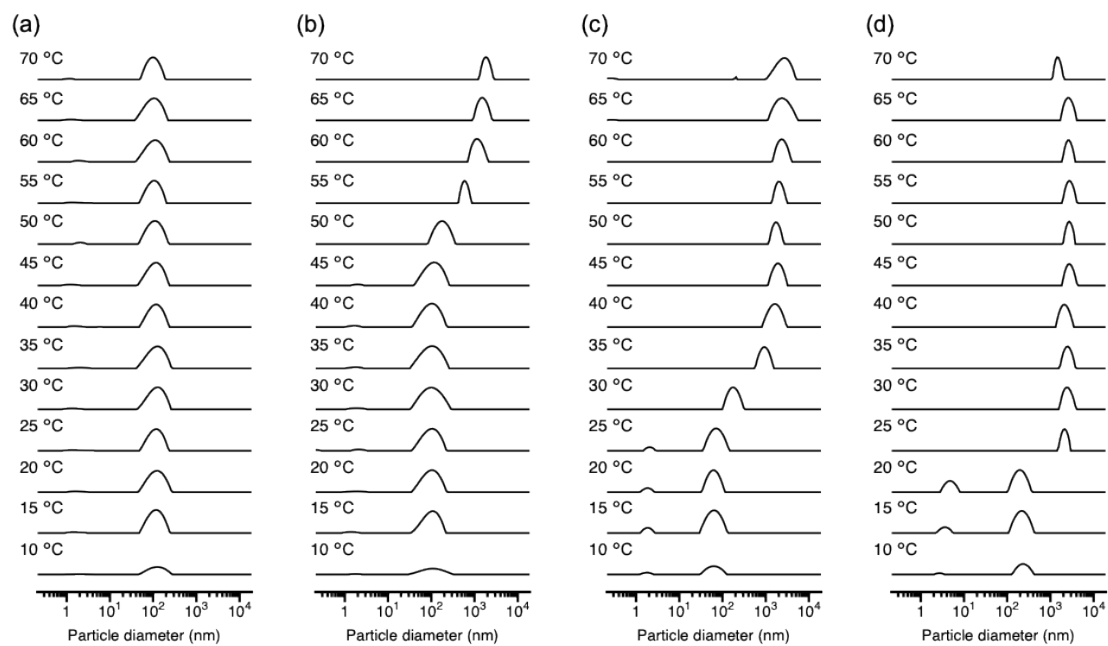


Figure S3. Temperature dependence of the particle size distributions in 3 wt% aqueous solutions of (a) **Me-DEG**, (b) **Et-DEG**, (c) **Pr-DEG**, (d) **Bu-DEG** measured by DLS method.

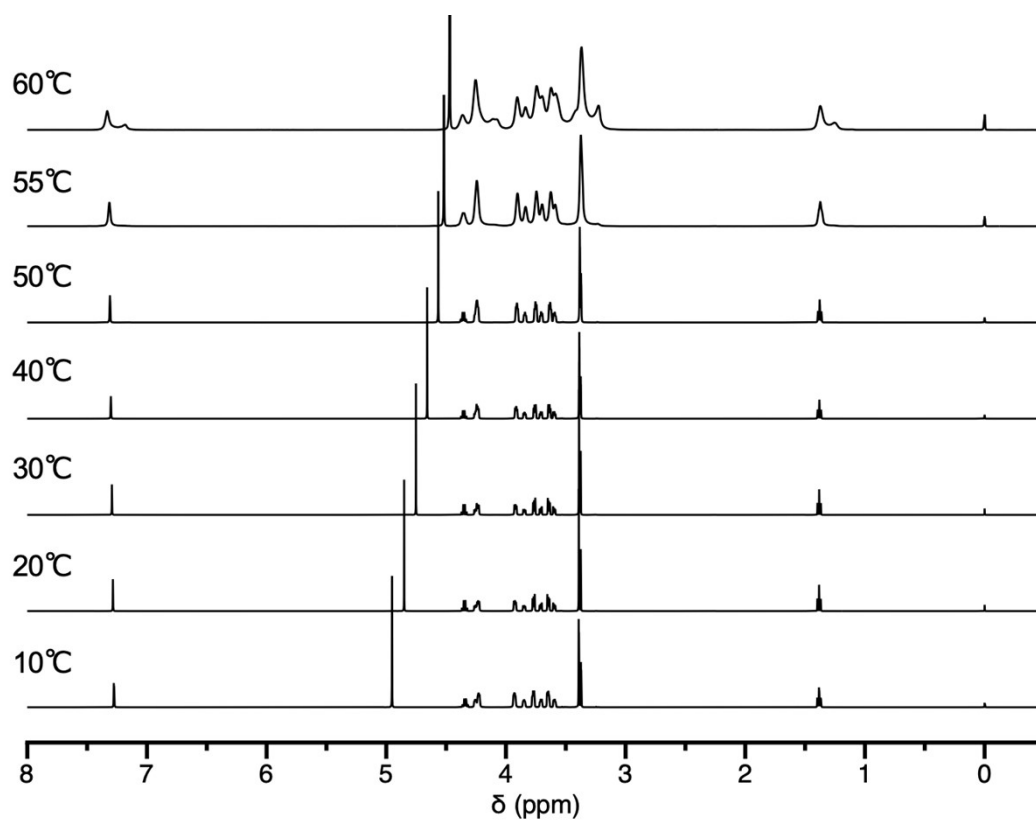


Figure S4. Temperature dependence of ^1H -NMR spectra of 3wt% **Et-DEG** in D_2O .

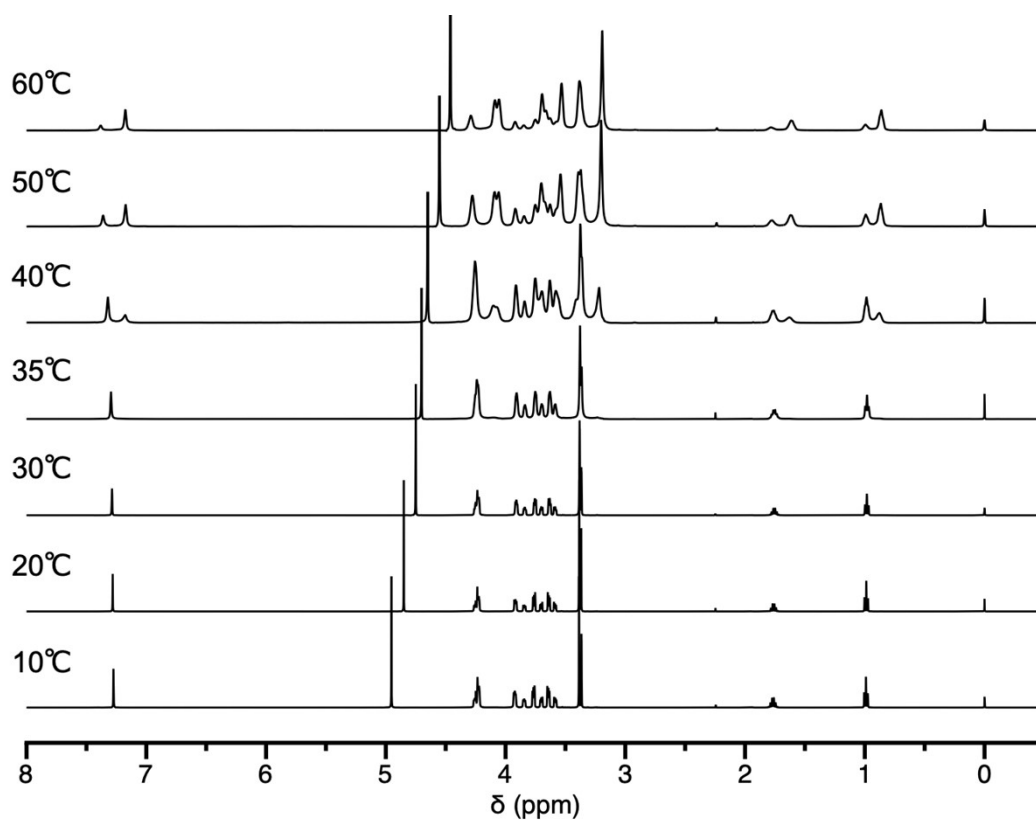


Figure S5. Temperature dependence of $^1\text{H-NMR}$ spectra of 3wt% **Pr-DEG** in D_2O .

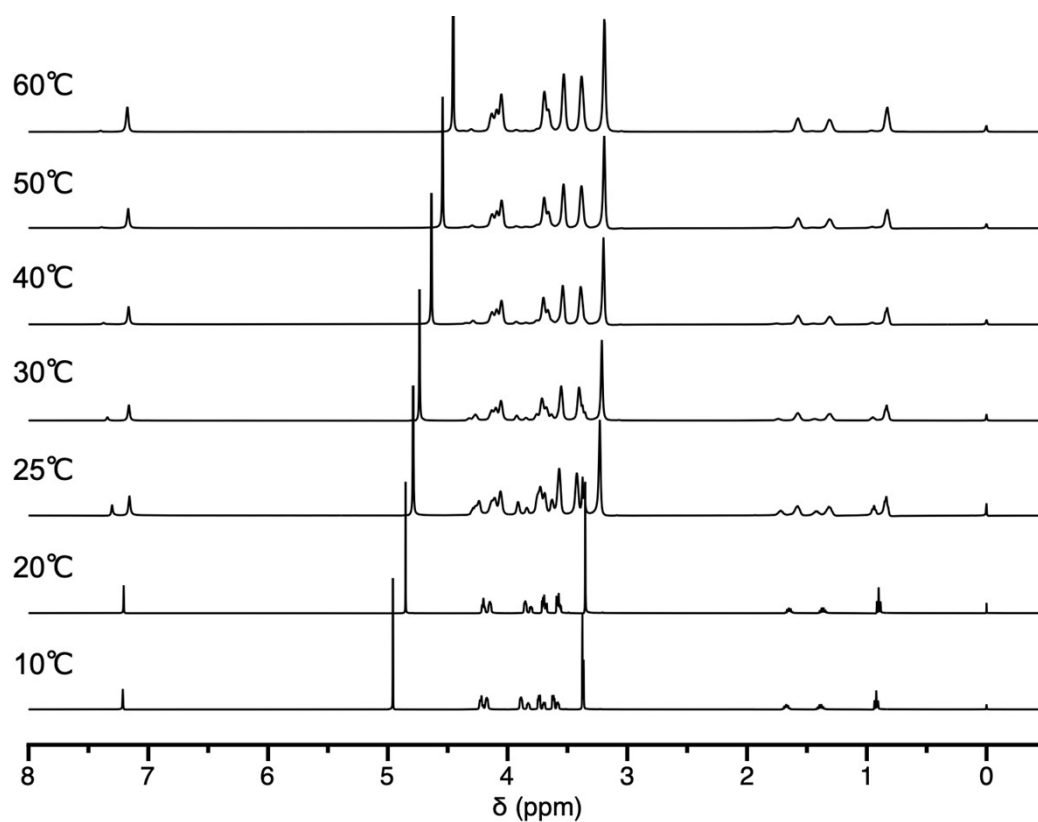


Figure S6. Temperature dependence of $^1\text{H-NMR}$ spectra of 3wt% **Bu-DEG** in D_2O .

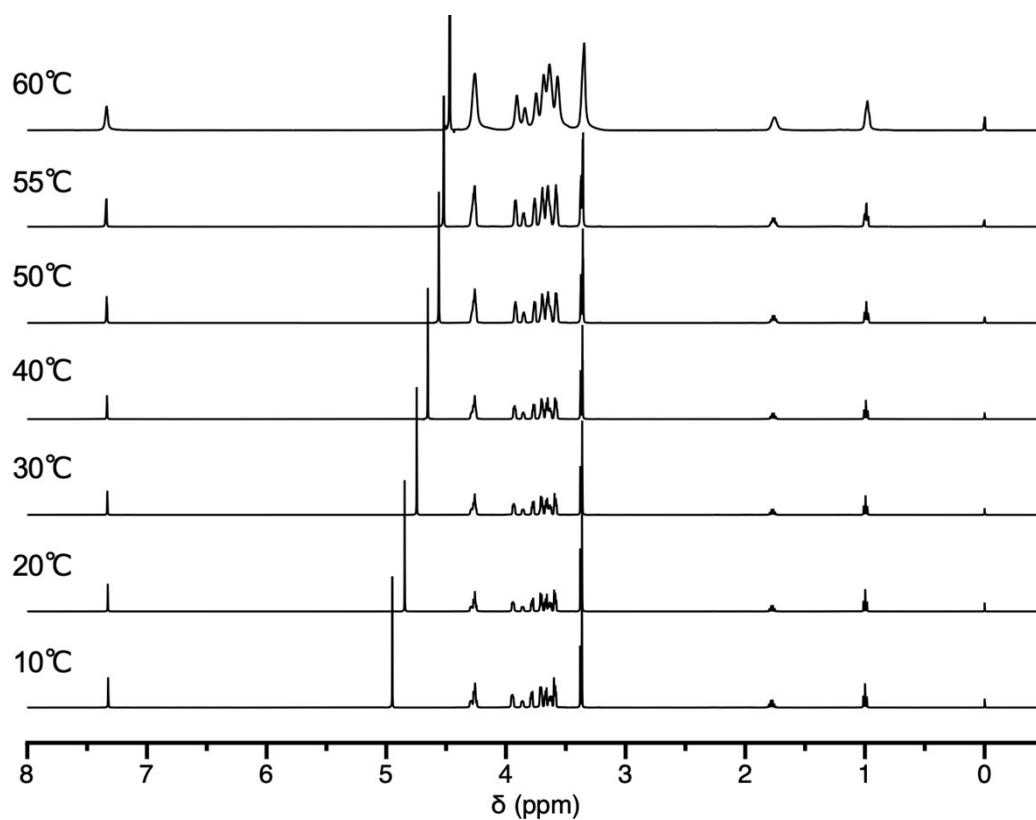


Figure S7. Temperature dependence of $^1\text{H-NMR}$ spectra of 3wt% **Pr-TEG** in D_2O .